Available online at www.sciencedirect.com

SciVerse ScienceDirect

Ceramics International 39 (2013) 3463–3478

CERAMICS INTERNATIONAL

www.elsevier.com/locate/ceramint

Review paper

The stability of $LiAlO_2$ powders and electrolyte matrices in molten carbonate fuel cell environment

Ermete Antolini*

Scuola di Scienza dei Materiali, Via 25 aprile 22, 16016 Cogoleto, Genova, Italy

Received 24 September 2012; received in revised form 20 October 2012; accepted 20 October 2012
Available online 9 November 2012

Abstract

The stability of $LiAlO_2$ electrolyte matrix is a key issue for the development of molten carbonate fuel cells (MCFCs). The phase transformation and particle growth of $LiAlO_2$ particles, observed after a long period of cell operation, is a serious problem and must be overcome in order to attain more than 40,000 h of MCFC life. This process is accompanied by pore size increase of the matrix, leading to a loss of capillary retention for electrolyte in the matrix, causing redistribution of electrolyte and finally resulting in the cross-over of gas. Therefore, efforts have been addressed to obtain a stable matrix with an appropriate pore structure and mechanical strength to provide effective gas-sealing properties without cracks formation during MCFC operation. This review deals on the chemical stability of $LiAlO_2$ powders in molten carbonates and the structural stability of $LiAlO_2$ matrices in MCFCs.

Keywords: C. Strength; E. Fuel cells; $LiAlO_2$; Phase transition

Contents

*Tel.: +39 0 109 182 880.
E-mail address: ermantol@libero.it

0272-8842/$ - see front matter © 2012 Elsevier Ltd and Techna Group S.r.l. All rights reserved.
http://dx.doi.org/10.1016/j.ceramint.2012.10.236

1. Introduction

Fuel cells are electrochemical devices, which convert chemical energy of electrochemical reactions directly into electrical energy. Molten carbonate fuel cell (MCFC) demonstrations have been able to show the highest fuel-to-electricity conversion efficiencies (> 50%) of any stand-alone fuel cell type. MCFC technology is more fuel flexible than lower temperature fuel cell technologies and is well suited for on-site stationary combined heat and power applications as well as to marine, military, and traction applications [1]. MCFCs consists of a porous nickel anode, containing dispersed chromium to provide strength and sintering resistance (fuel electrode), a porous, lithium-doped, nickel oxide cathode (oxidant electrode), and a lithium aluminate matrix filled with lithium and potassium or sodium carbonates (50–70 mol% Li_2CO_3) as the electrolyte. The cell is operated at a temperature of about 650 °C and at a pressure of 1–10 atm; the fuel gas is a humidified mixture of H_2 and CO, and the oxidant is a mixture of O_2 and CO_2 which may contain water vapor [2–4]. It is generally assumed that a stack lifetime of atleast 40,000 h is required in order to achieve cost of electric targets, provided that the system is used for co-generation [4]. It is well known that the lifetime limiting issues for MCFC systems are mainly materials issues of the stack. Dissolution of NiO cathode material, corrosion of separator plates, electrolyte losses, electrolyte retention capacity, catalyst deactivation (in the case of internal reforming), matrix cracking, high temperature creep of porous components and contaminants are the main lifetime limiting constraints [5,6]. Therefore improvement in endurance of the MCFC stack and its components is an important issue in the worldwide research and development of MCFC.

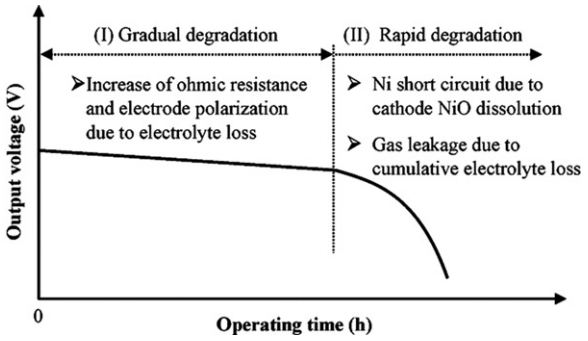

Fig. 1. Schematic diagram of MCFC degradation according to operating time (at a constant current). Reprinted from Ref. [7] copyright 2010, with permission from Elsevier.

The voltage degradation of a MCFC is generally divided into two phases as shown in Fig. 1 [7]. The first phase shows a gradual degradation caused by the increase of ohmic resistance (i.e. internal resistance) and the electrode polarization due to the carbonate electrolyte loss. The second phase shows a rapid degradation, which may be caused by Ni short circuit or the gas cross leakage between the electrodes due to the cumulative electrolyte loss over the long period. The transfer from the first phase to the second phase determines the period of operating of a MCFC power unit.

In a previous work, the stability of molten carbonate fuel cell electrodes has been reviewed [8]. Another key point affecting the durability of a MCFC is the amount of electrolyte in the cell. It is well known that one of the major causes of the deterioration of MCFCs is electrolyte depletion. Indeed, the cell performance depends greatly on the amount

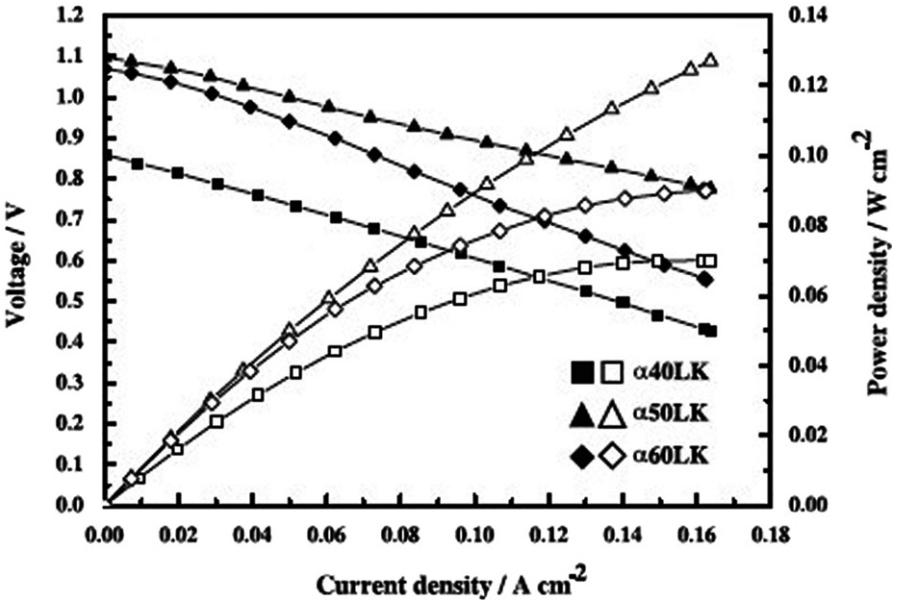

Fig. 2. Polarization and power density curves in single MCFC with different Li_2CO_3/K_2CO_3 (62/38 mol%) electrolyte content in α-$LiAlO_2$ matrices. Anode: Ni alloy. Cathode: in-situ lithiated NiO. Full symbols: polarization curves; open symbols: power density curves. Reprinted from Ref. [9] copyright 2011, with permission from Elsevier.

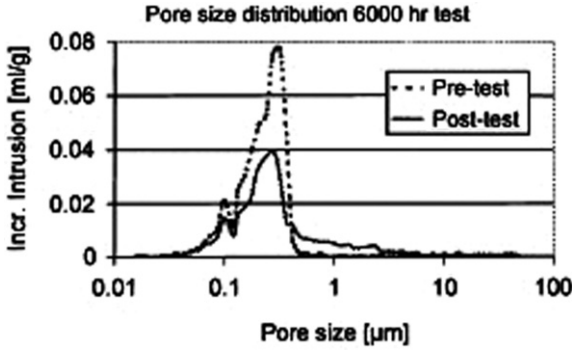

Fig. 3. Pore size distribution of matrix before and after 6000 h stack experiment. Reprinted from Ref. [10] copyright 2000, with permission from Elsevier.

of electrolyte in the cell. As can be seen in Fig. 2 [9], the MCFC unit cell with 50% (α50LK) and 60% (α60LK) volume fractions of Li_2CO_3/K_2CO_3 exhibited higher open circuit voltage (OCV) values (1.09 and 1.06 V, respectively) than that of the cell with 40% volume fraction of electrolyte (α40LK) (0.85 V), due to the shortage of electrolyte material. The power density of α50LK and α60LK cells was higher than that the α40LK cell, however, the α60LK cell, in which an excess of electrolyte material is present, showed a lower performance than the α50LK, due to the increase in electrode resistance. Lithium aluminate, the state-of-the-art matrix support material, plays the role of maintaining the amount of electrolyte in the matrix at an appropriate level. It should have an appropriate pore structure and mechanical strength to provide effective gas-sealing properties without cracks forming in the matrix during MCFC operation. The phase transformation and particle growth of $LiAlO_2$ particles, observed after a long period of cell operation, is a serious problem and must be overcome in order to attain more than 40,000 h of MCFC life. This process is accompanied by pore size increase of the matrix, as can be seen in Fig. 3 [10]. This can lead to a loss of capillary retention for electrolyte in the matrix, causing redistribution of electrolyte and finally resulting in the cross-over of gas [10]. Therefore, efforts have been addressed to obtain a stable matrix with an appropriate pore structure and mechanical strength to provide effective gas-sealing properties without cracks formation during MCFC operation. This review deals on the chemical stability of $LiAlO_2$ powders in molten carbonates and the structural stability of $LiAlO_2$ matrices in MCFCs.

2. Chemical stability of $LiAlO_2$ powders in molten carbonates

2.1. General overview

At least three different crystal structures, that is, α, β and γ, are known for $LiAlO_2$. The α phase is the low-temperature stable polymorph, hexagonal with space group *R*-3*m*, lattice parameters $a=2.799$ Å and $c=14.180$ Å, and the density of 3.401 g cm^{-3} [11]. The γ phase is the high-temperature stable one, tetragonal with lattice parameters $a=5.169$ Å and $c=6.268$ Å, space group $P4_12_12$ and a density of 2.615 g cm^{-3} [12]. The β phase is always metastable, orthorhombic with lattice parameter $a=5.280$ Å, $b=6.300$ Å and $c=4.900$ Å, space group $Pna2_1$ and a density of 2.685 g cm^{-3} [13]. Phase transformation between α-$LiAlO_2$ and γ-$LiAlO_2$ may occur during operation of the MCFCs. In particular, considering the fact that there is a substantial difference in the density between α-$LiAlO_2$ and γ-$LiAlO_2$, this phase transformation may cause a change in the pore size distribution of the matrix. Data concerning the thermodynamic phase diagram for $LiAlO_2$ crystal structures have been proposed by Byker et al. [14], where the stable crystal structure under an air atmosphere condition was determined in terms of bulk pressure and temperature. According to this diagram, the stable crystal structure at atmospheric pressure and a temperature of 650 °C, which is typical for the operating condition of MCFCs, is the γ-$LiAlO_2$ structure. Because of its thermal stability, initially, in MCFCs, submicron γ-$LiAlO_2$ powder was used as the electrolyte-retaining material. More recently, Danek et al. [15] investigated the occurrence of α→γ-$LiAlO_2$ phase transformation under atmospheres of CO_2 and N_2, both dehydrated and water vapour containing, at temperatures of 800, 850 and 900 °C, in the α-$LiAlO_2$ powder. An increasing of γ-$LiAlO_2$ phase concentration in the α-$LiAlO_2$ sample was observed, depending on temperature and time of heating the sample. The results of this investigation suggested the existence of some chemical steps of the overall phase transformation process, probably the decomposition of the oxide at the α-$LiAlO_2$ particle surfaces via a surface-nucleation mechanism. This transformation, however, did not take place below 700 °C, which is the upper temperature limit of the MCFC operation. However, the concomitant effects of molten carbonate and CO_2 present in real fuel cell operating conditions on $LiAlO_2$ phase transformation were not take into account. In addition to phase transition,

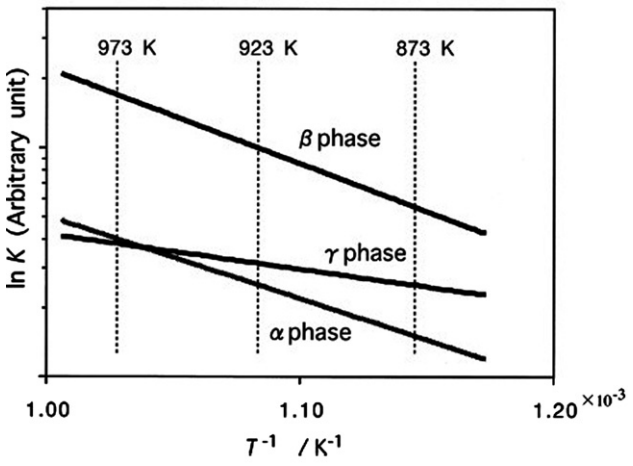

Fig. 4. Equilibrium constant of dissolution reaction of $LiAlO_2$ (predicted line). Reprinted from Ref. [16] copyright 1998, with permission from Elsevier.

dissolution of $LiAlO_2$ occurs in molten carbonate, as the following reaction [16]:

$$LiAlO_2 + CO_3^{2-} \rightarrow Li^+ + CO_2 + AlO_3^{3-} \quad (1)$$

As can be seen in Fig. 4 [16], the logarithm of the equilibrium constants K of the dissolution reaction of α-, β- and γ-$LiAlO_2$ is proportional to the reciprocal of the absolute temperature. The equilibrium constants of the dissolution reaction of α-, β- and γ-$LiAlO_2$ are in the order $K_\beta > K_\alpha > K_\gamma$ at temperatures > 700 °C and $K_\beta > K_\gamma > K_\alpha$ at temperatures < 700 °C [16]. It has to be underlined that the phase transformation and the particle growth of lithium aluminate are strongly correlated to its solubility in molten carbonates. A lot of works on the stability of α- and γ-$LiAlO_2$ have been carried out in the presence of molten carbonates. Initially, an eutectic mixture of Li_2CO_3 and K_2CO_3 was used as the electrolyte in MCFCs, then K_2CO_3 was generally substituted by Na_2CO_3, being the NiO cathode less soluble in Na_2CO_3 than in K_2CO_3 [8]. In the following sections the stability of $LiAlO_2$ in Li/K and Li/Na carbonates was separately reviewed.

2.2. Chemical stability of $LiAlO_2$ in Li/K carbonates

Stability tests in Li/K carbonates have been carried out on the different $LiAlO_2$ phases both out-of-cell and in a single MCFC. Terada et al. [16] carried out immersion tests in Li/K (62/38) carbonate eutectic at 650 °C for 500 h on a mixture of α- and γ-$LiAlO_2$. In air, the α phase was converted to the γ phase. In CO_2 atmosphere, instead, the α phase did not appear to transform to the γ phase. The effect of temperature on the stability of a α-, β- and γγ-$LiAlO_2$ mixture in Li/K carbonates was also investigated: the β phase decreased throughout the range 600 to 650 °C. The α phase increased significantly between 600 and 650 °C and decreased at 700 °C. The γ phase increased significantly at 700 °C. From this viewpoint, the transformation temperature from the α phase to the γ phase, and vice versa, is considered to be between 650 and 700 °C. Thus, it was suggested that α-$LiAlO_2$ should be an appropriate electrolyte support for a MCFC operating at around 650 °C. A group at Tokyo Electric Power Company carried out equilibrium solubility measurements of lithium aluminate in Li/K molten carbonates under various conditions and investigated the mechanism of γ-$LiAlO_2$ particle growth in Li/K carbonates [17,18]. The results indicated that particle growth depends on the basicity of the electrolyte [17]. Although the particles mainly grow through a dissolution-precipitation mechanism, with γ-$LiAlO_2$ passing through the molten carbonate, growth tends to occur readily in the interior of agglomerates resulting from the coagulation of fine particles. As fine pores fill fully with γ-$LiAlO_2$ precipitate in the interior of the agglomerates, and then are amalgamated into other surrounding particles, the particles can grow at higher rates than individual particles, which grow by the dissolution-precipitation mechanism [18]. Terada et al. [16] reported that particle growth occurs faster at higher temperature and in low CO_2 gas atmospheres, in agreement to $LiAlO_2$ dissolution by Eq. (1). According to Zhou et al. [19], the α-$LiAlO_2$ matrix porosity impregnated with Li/K eutectic carbonate increased with the sintering time at 650 °C under N_2, due to both the rearrangements of the α-$LiAlO_2$ particles and the dissolution–slight deposition of the α-$LiAlO_2$ microparticles. In contrast, those sintered without impregnating with the electrolyte were affected only by rearrangements, but not by dissolution–slight deposition. Accompanying the rearrangements of the α-$LiAlO_2$ particles, the dissolution–slight deposition of the α-$LiAlO_2$ microparticles resulted in an additional enlargement of the micro pore diameter and the mean pore diameter, leading to a narrow pore-size distribution in the matrices during their sintering process. Takizawa and Hagiwara [20] studied the reciprocal effect of phase transformation and dissolution: they investigated in detail the phase transformation between the α-$LiAlO_2$ and γ-$LiAlO_2$ in molten Li/K carbonate at 650 °C in air or CO_2, taking into account of both the effect of the solubility of crystal structure and the particle size, that is, the solubility of α-$LiAlO_2$ in Li/K carbonates is different than that of γ-$LiAlO_2$, and the fine particles dissolve more easily than larger particles. The results of their experiments are summarized in Table 1. The overall phenomena are the following: small-size particles dissolve in molten carbonate and deposit onto the surfaces of large-size particles, the growth rate of γ-$LiAlO_2$ particles in molten carbonate

Table 1
Conditions for $LiAlO_2$ phase transition (α→γ, γ→α) and/or particle growth (α→α, γ→γ) [20].

Atmosphere	Phase	Particle size	α-$LiAlO_2$		γ-$LiAlO_2$	
			α→α	α→γ	γ→γ	γ→α
Air	Single	—	X[a]	O[b]	O	X
CO_2	Single	—	O	X	O	X
	Mixed	Small (α=γ)	O	X	O	X
	Mixed	Large (α=γ)	X	X	X	O
	Mixed	α>γ	X	X	X	O
	Mixed	α<γ	X	O	X	X

[a] X Phase transition or particle growth does not occur.
[b] O Phase transition or particle growth occurs.

Table 2
Characteristics of $LiAlO_2$ in the matrix following different MCFC operating times [23].

Operating time	Particle growth (μm)	α-$LiAlO_2$ amount (%)
Start of test	0.1–0.5	0
15,000 h	0.4–4.0	31
40,000 h	0.5–8.0	80

is extremely large in comparison to that of α-$LiAlO_2$, γ-$LiAlO_2$ is more stable than α-$LiAlO_2$ under air atmosphere, while under CO_2 and in the absence of particle size effect the solubility of α-$LiAlO_2$ is lower than that of γ-$LiAlO_2$. The difference in growth rates between the two phases becomes especially pronounced at high temperature and low CO_2 partial pressure, conditions which accelerate the growth of $LiAlO_2$ particles. Very recently, Patil et al. [21] carried out immersion tests in molten eutectic Li/K carbonate mixture at 650 °C on γ-$LiAlO_2$ and α-$LiAlO_2$ to evaluate the phase and microstructure stabilities of these materials. The γ-$LiAlO_2$ phase transformation was dependent on the immersion time. The presence of the α-$LiAlO_2$ after immersion tests phase revealed that phase transformation of γ-$LiAlO_2$ occurs in Li/K carbonate melts under cathode gas atmospheres; in contrast, no phase transformation was evident after immersion of the pure α-$LiAlO_2$ phase in molten carbonate for 5000 h. Summarizing, different immersion tests in Li/K carbonates essentially indicated the α-phase is stable in a low-temperature (≤ 650 °C) and high CO_2 pressure environment, whereas the γ-phase is stable in a high-temperature (> 650 °C) and low CO_2 pressure environment [22].

Stability tests in MCFCs with Li/K eutectic carbonate mixture have been performed on γ-$LiAlO_2$ [23] and α-$LiAlO_2$ [24] matrices. Tanimoto et al. [23] tested a γ-$LiAlO_2$ matrix on a single MCFC for 15,000 and 40,000 h. Table 2 shows the characterization of γ-$LiAlO_2$ both before and after testing. The particle size of γ-$LiAlO_2$ increased with operating time. It was suggested that there is a decreased in both the specific surface area and the electrolyte supporting force of the matrix. The crystal phase of $LiAlO_2$ changed from the γ- to the α-phase with time; 31 and 80% of γ-$LiAlO_2$ was transformed to the α-phase after 15,000 and 40,000 h, respectively. Batra et al. [24] carried out a short duration test using α-$LiAlO_2$ as the matrix material in a single MCFC. The cell test gave satisfactory performance with a maximum open-circuit voltage of 1000 mV and a stable value in the range 850–1000 mV for more than 10 h. Clearly, to assess the stability of the α-$LiAlO_2$ matrix in MCFCs operating with Li/K carbonate eutectic long-term duration tests must be carried out.

2.3. Chemical stability of $LiAlO_2$ in Li/Na carbonates

As can be seen in Fig. 5, the solubility of γ-$LiAlO_2$ in eutectic Li/Na carbonate mixture is approximately three times as large as that in eutectic Li/K carbonate mixture [25]. Different acid–base equilibria in these two molten electrolytes affect the solubility of $LiAlO_2$. Therefore, in the former electrolyte, one can expect a greater reactivity of $LiAlO_2$ particles than in the latter. At 650 °C in Li/Na carbonate mixture, α-$LiAlO_2$ is regarded to be more stable than γ-$LiAlO_2$ from out-of-cell tests, and is supposed to have lower solubility than γ-$LiAlO_2$ [25]. γ-$LiAlO_2$, which is relatively unstable and has higher solubility, is supposed to dissolve into the carbonate and to precipitate as α-$LiAlO_2$ during cell operation. Immersion tests in molten Li/Na carbonates were performed in air for different times up to 18,000 h at 650 °C on an α-/γ-$LiAlO_2$ (1:1) mixture [26]. The increase of the α-$LiAlO_2$ to γ-$LiAlO_2$ intensity ratio of XRD reflexions with thermal treatment time indicated the higher stability of the α-phase (see Fig. 6).

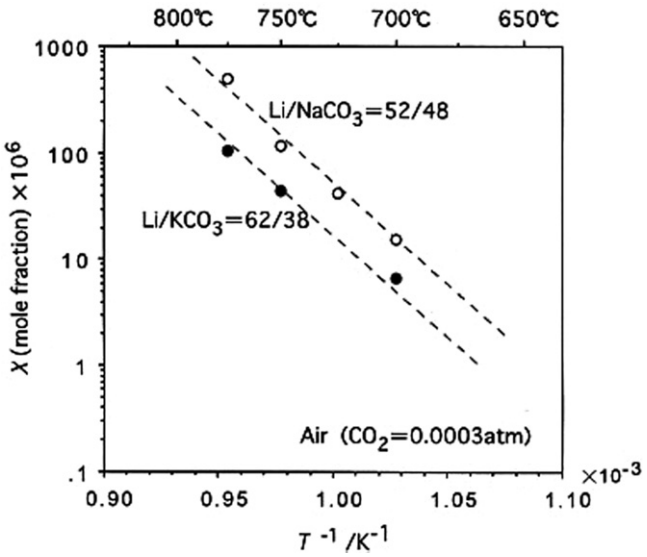

Fig. 5. Effect of carbonate composition on solubility of γ-$LiAlO_2$. Reprinted from Ref. [25] copyright 1999, with permission from Elsevier.

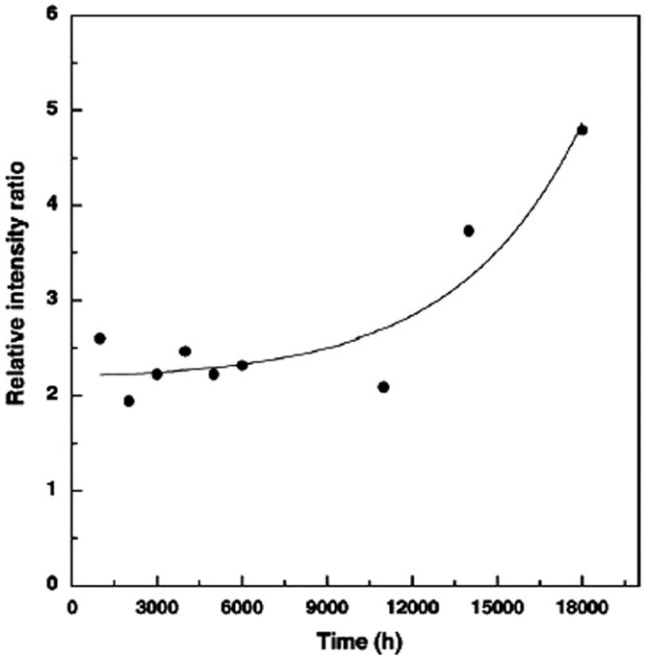

Fig. 6. Variation with heat-treatment time of the α-$LiAlO_2$ to γ-$LiAlO_2$ intensity ratio of XRD reflexions from an α-/γ-$LiAlO_2$ mixture (1:1) in molten Li/Na carbonate at 650 °C. Reprinted from Ref. [26] copyright 2005, with permission from Elsevier.

Within the temperature range of 600–700 °C, the reaction:

$$Al_2O_3 + Li_2CO_3 \rightarrow 2LiAlO_2 + CO_2$$

is strongly shifted to the right, and is the basis of the methods of the $LiAlO_2$ synthesis. Suski and Tarniowy [27] addressed a study to the identification of the crystallographic form of $LiAlO_2$, produced in reaction (2) within the MCFC operation temperature range as well as the solid phase transformation, in excess of molten eutectic Li/Na carbonate. They expected that the thermodynamically stable crystallographic form of $LiAlO_2$ should appear in course of this reaction. Therefore, they assumed that even if the α-$LiAlO_2$ is the first product of

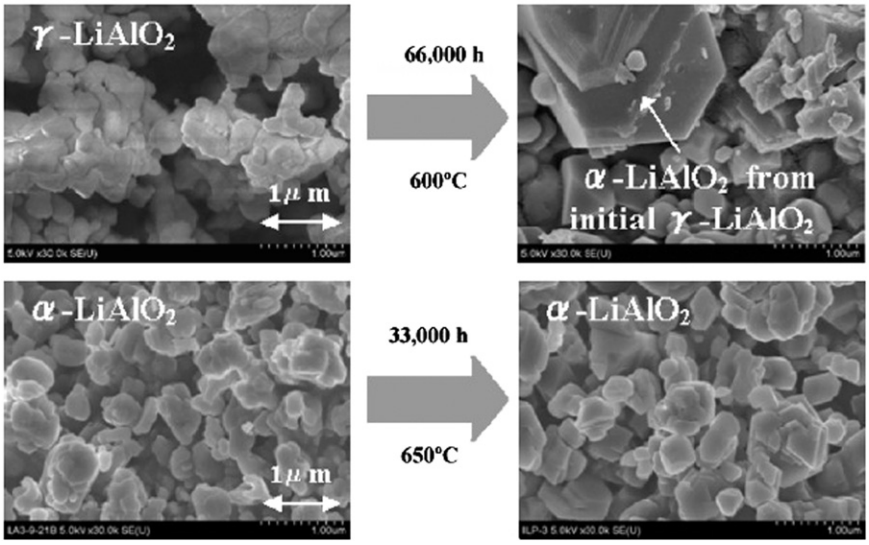

Fig. 7. Electrolyte matrix images before and after the operation using SEM. Reprinted from Ref. [7] copyright 2010, with permission from Elsevier.

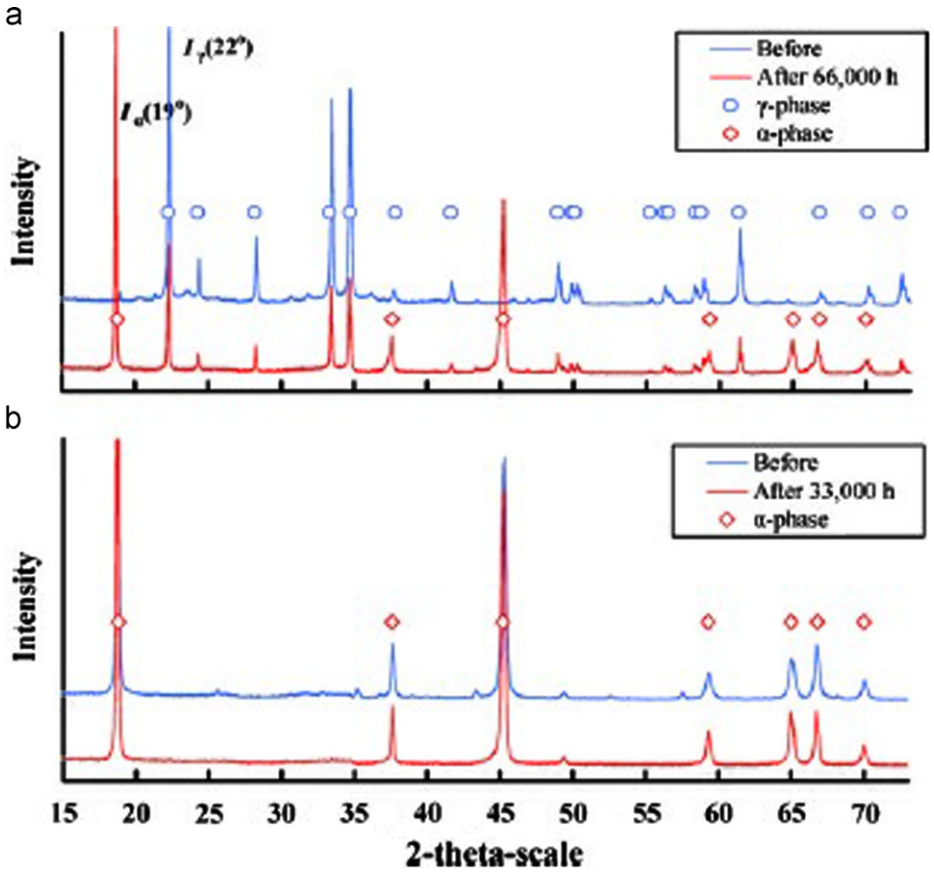

Fig. 8. X-ray diffraction patterns of the $LiAlO_2$ matrix before and after the operation: (a) 600 °C–66,000 h operation; (b) 650 °C–33,000 h operation. Reprinted from Ref. [7] copyright 2010, with permission from Elsevier.

reaction (2), the γ-phase, if it is really stable at these temperatures, should appear already before the conversion according to reaction (2) is complete. The reaction (2) was carried out on mixtures with stoichiometric initial ratios of Al_2O_3 to Li_2CO_3, as well as on those containing an excess of 38 mol of Li_2CO_3/Na_2CO_3 (53/47) eutectic. The results indicated that at 600–700 °C, when produced by the reaction of solid Li_2CO_3 with Al_2O_3, as well as in the presence of molten Li/Na carbonates, $LiAlO_2$ appears in the α-crystallographic form. This conclusion is consistent with observation of some partial conversion of the γ to α-$LiAlO_2$ phase in the MCFC after a long operation of the cell. The rate of such conversion, however, is probably very slow and the γ-$LiAlO_2$, commonly used as the solid component of the MCFC electrolytic tiles, may be easily considered as apparently stable at the MCFC operation temperature. Indeed, conflicting results on the stability of γ-$LiAlO_2$ during long-term MCFC operation with Li/Na carbonates have been reported. Fujita et al. [28] analyzed the degradation of the γ-$LiAlO_2$ matrix after long-term operation of MCFCs with the Li/Na carbonates. There were no detectable differences on both $LiAlO_2$ particle size and phase composition between the matrices before and after long-term operation. On the other hand, Morita et al. [7] carried out stability tests on γ- and α-$LiAlO_2$ matrix during long-term operation in MCFC with Li/Na carbonates. Fig. 7 shows SEM images of the matrix before and after the operation of the 600 °C–66,000 h and the 650 °C–33,000 h MCFCs. By comparing the morphology and particle size of $LiAlO_2$ particles before and after the operation, the α-$LiAlO_2$ particles of the 650 °C–33,000 h cell only shows a slight change after the operation, whereas the γ-$LiAlO_2$ particles of the 600 °C–66,000 h cell shows severe changes after the operation with a lot of large and coarse particles. Fig. 8 shows the X-ray diffraction patterns of the $LiAlO_2$ matrix before and after the operation. The XRD patterns of the α-$LiAlO_2$ show no changes between before and after the operation and maintain their initial pattern even after the 650 °C–33,000 h operation. On the other hand, the XRD patterns of the γ-$LiAlO_2$ before and after the operation show a phase change from the initial γ to α. Approx. 70% of the initial γ-$LiAlO_2$ changed into α-$LiAlO_2$ after the 600 °C–66,000 h operation. The results of the XRD patterns suggest that the small initial γ-$LiAlO_2$ are transformed in large and coarse α-$LiAlO_2$ particles.

Summarizing, at 650 °C and in CO_2 atmosphere α-$LiAlO_2$ seems to be more stable than γ-$LiAlO_2$ in both Li/K and Li/Na carbonates.

2.4. Methods to improve $LiAlO_2$ stability in molten carbonates.

The effect of additives on inhibiting particle growth and phase transformation of $LiAlO_2$ has been investigated. Yasumoto et al. [29] found that the electrolyte retention ability of a $LiAlO_2+ZrO_2$ mixture is higher than that of bare $LiAlO_2$. Following immersion in molten Li/Na carbonates under 10% CO_2/90% air atmosphere for

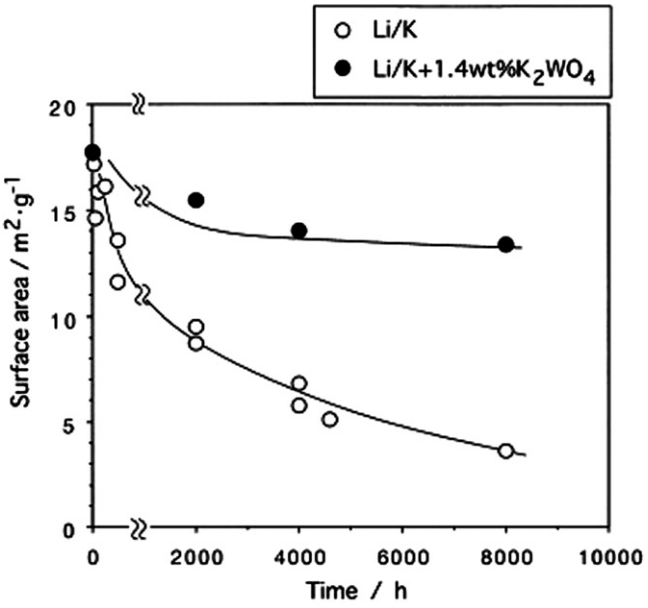

Fig. 9. Changes in surface area of HSA-19, undoped and doped with potassium tungstate at 650 °C, Li/K, 30% CO_2/70% air. Reprinted from Ref. [16] copyright 1998, with permission from Elsevier.

4000 h the decrease of the specific surface area of $LiAO_2/ZrO_2$ was lower than that of $LiAlO_2$ alone. The $LiAO_2/ZrO_2$ particles grew more slowly compared with bare $LiAlO_2$. Among different candidate materials, potassium tungstate was the most effective to stabilize $LiAlO_2$ in the 500-h immersion test in molten Li/K carbonates [16,30]. It was found that the addition of potassium tungstate can inhibit both the particle growth and the phase transformation of HSA-19 (a mixture of α-, β- and γ-$LiAlO_2$ powder). As can be seen in Fig. 9 [16], the change with time of the surface area of HSA-19 doped with potassium tungstate was lower than that of undoped $LiAlO_2$. The phase transformation of $LiAlO_2$ at CO_2 ambient is shown in Fig. 10 [30]. In the absence of tungstate an increase in the α-phase and a decrease in the β- and γ-phases was observed. Conversely, in the presence of 1.4 wt% K_2WO_4 the corresponding changes in the relative phase amount were small.

3. Matrix fabrication

An important characteristics of the matrix is its mechanical strength. MCFC matrices are usually fabricated to have a porosity of 50–60% and a pore size below 1 μm using microsized $LiAlO_2$ powders [31]. The submicron α-$LiAlO_2$ powder in the matrix is the current preferred material choice [5]. The electrolyte matrix has to remain substantially crack-free in order to provide effective gas-sealing properties during MCFC operation. During initial start-up and operation of a MCFC stack, the matrix experiences both mechanical and thermal stresses as a result of the difference between the thermal expansion

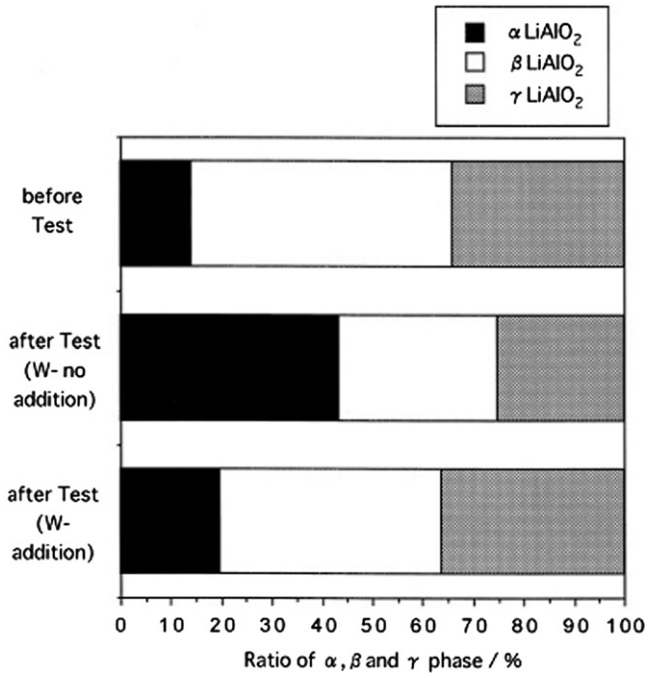

Fig. 10. Influence of tungstate addition on phase transformation of $LiAlO_2$ at 650 °C–500 h operation in Li/K eutectic carbonate under CO_2. Reprinted from Ref. [30] copyright 1999, with permission from Elsevier.

coefficients of the $LiAlO_2$ ceramic particles and the carbonate electrolyte. More particularly, the difference in thermal expansion coefficients between the $LiAlO_2$ ceramic particles (less than $10 \times 10^{-6}\,°C^{-1}$) and the carbonate electrolyte (greater than $20 \times 10^{-6}\,°C^{-1}$) can generate a significant amount of compressive stress on the $LiAlO_2$ particles and tensile stress on the carbonates during cooling. Therefore, even in the absence of mechanical stress, the thermal stress generated by the thermal expansion mismatch is sufficient to cause cracking of the matrix during thermal cycling. The matrix cracking during either start-up or operation permits undesired fuel and oxidant gas cross leakage, causing lower power generation efficiency, shorter life and, more importantly, poor power plant economy.

The matrix is generally prepared by tape casting using a non-aqueous slurry. The binder and plasticizer are polyvinyl butyral (PVB) and polyethylene glycol, respectively, and the solvent is a mixture of butanol and *iso*-propyl alcohol. The burn process of the organic compounds in the matrix affects its physical parameters and MCFC performance. Different studies were addressed to the thermal decomposition of PVB [32–34], observing complicated decomposition products. Lin et al. [35] studied the dependence of the volatilization of the organic additives and the burn of PVB on the micro-pore configurations in the cell matrix. The micro-pore configurations with a large amount of micro-pores in the cell matrix before the burn of the organic compounds promoted the volatilization of the organic additives and the burn of PVB. The smooth diffusion of oxygen through a large amount of the micro-pores including new and old ones was responsible for the complete burn of PVB. The smooth volatilization of the organic additives and the complete burn of PVB in the cell matrix were the more significant factors for the improved MCFC performance.

To determine the change in characteristics due to heating and binder burn out, Batra et al. [24] heated pieces of green tapes with various ceramic content (47–59 wt%) at 650 °C in air. The slurry composition with 56 wt% ceramic was chosen for scale-up to obtain tapes for cell testing. The larger tapes (15 cm × 30 cm) of this composition however developed cracks during drying. Therefore, scaling-up was attempted with a lower ceramic content of 52 wt%. This composition resulted in satisfactory large tapes. The matrix has sub-micron pores in the range 0.2–0.9 μm and a porosity of 70 vol%.

To obtain more appropriate slurry formulation, compositions with different ceramic content (42, 50 and 54 wt%) were characterized after burning out the binders at 650 °C [36]. The final density increased with increasing ceramic content. This is expected since the particles would be closer packed with increasing solid content in the slurry. The 54 wt% sample presented mostly submicron pores in the range 0.1–1 μm, while the 42 wt% sample had a bimodal distribution with pores in the sub-micron (0.07–0.6 μm) and micron (2–6 μm) range. The larger pores in 42 wt% ceramic sample could result from volatilisation of a larger quantity of organic additives. The earlier results indicate that the ceramic content of the slurry influences the porosity as well as pore size distribution of the matrix; higher ceramic content leads to narrower pore size distribution and optimum porosity.

4. Mechanical strength of $LiAlO_2$ matrices: methods for increasing crack resistance and mechanical strength of the matrix

Various approaches for improving the crack resistance and mechanical strength and extending the life of the electrolyte matrix have been proposed. A number of these approaches are based on incorporating secondary reinforcing phases into the matrix, in the form of refractory metallic alloys, large particles, fibers, rod-shaped γ-$LiAlO_2$ particles, low melting metal powders and metal wire mesh. They act as either crack attenuators and deflectors to slow crack propagation or to enhance the bonding between the ceramic support materials, resulting in improved matrix strength and toughness.

4.1. Refractory metallic alloys

Arendt and Curran [37] used refractory metallic alloys as the reinforcement material for the $LiAlO_2$ matrix. These alloys consisted of a major amount of Fe (about 75 wt%) alloyed with Cr, Al and Co. This reinforcement can be in a

number of forms such as a fine screen, fibers or woven mesh, in a volume ranging from about 1% to about 6% by volume of the matrix.

4.2. Ceramic particulates and fibers

The predictions of Faber and Evans [38] provided the basis for design of a high toughness two-phase ceramic materials. The ideal second phase, in addition to maintaining chemical compatibility, should be present in amounts of 10–20 vol%. Greater amounts may diminish the toughness increase due to overlapping particles. Particles with high aspect ratios are most suitable for maximum toughening [37]. Ceramic particulates and fibers have been proposed for reinforcing MCFC matrix. The choice of materials stable in carbonates is rather limited. Strong commercial ceramic fibers, such as Al_2O_3, may not have sufficient long-term stability in carbonate electrolyte. The γ-$LiAlO_2$ fibers are expected to be stable in carbonate, but may be nonuniform, defective and weak in structure. The mechanical property requirements for the ceramic particulates, instead, are less stringent, although the incorporation of the particulates may be less effective. Nevertheless, the particulates are a lower cost alternative to the fibers. The considerations for material selection include strengthening potential, stability and cost. In terms of cost, expensive single-crystal whiskers or fibers are not considered. Porosity and nonuniformity are not acceptable for fibers because they severely degrade fiber strength. High silica content is also not acceptable because silica not only enhances the formation of weak glassy grain boundaries, but also dissolves in carbonate as silicate. Al_2O_3 and ZrO_2 materials may be usable, provided that protective lithiated surface oxide layers can form. On this bases, Yuh et al. [39] tested matrices incorporating different materials (including fibers and particulates of Al_2O_3, ZrO_2, $LiAlO_2$, etc.) as reinforcements in single MCFCs. All these cells showed significant improvements by the additives in maintaining matrix seal efficiency during thermal cycling. The fiber strengthened matrices thermal cycled better than both the particulate ones and the additive-free matrix.

4.2.1. Large particles

Bushnell et al. [40] incorporated into a single MCFC and cycled between operating temperature and room temperature a matrix formed by 90 vol% submicron $LiAlO_2$ support particles and 10 vol% alumina crack attenuator particles with an average size of 100 μm. The presence of the larger particles resulted in thousands of discontinuous microcracks being formed throughout the matrix as it cools down from operating temperature to room temperature. Evidently, the stresses resulting from the electrolyte phase change and differential thermal expansion between components during cool down are relieved through the formation of this multitude of tiny discontinuous cracks, rather than by the formation of one or more large thru-cracks. Upon reheating to operating temperature the microcracks heal themselves such that, in tests conducted to date, no noticeable permanent damage occurs during a cycle. Therefore, the matrix can be continuously recycled with no detrimental effect. Vine et al. [41] proposed a flexible and pliable MCFC matrix, formed by three components, that is, fine inert particulate material (γ-$LiAlO_2$), larger crack attenuating ceramic particulate material, and an organic polymeric binder (commonly polyvinyl butyral), which is removed during the fuel cell start-up. The crack attenuator of the tape is corrosion resistant ceramic particulate material having an average size range greater than about 50 μm. It can be made of the same material as the inert particles above, or a more reactive material such as alumina which, because of the larger particle size, has less surface area and, therefore, less reactivity toward the molten carbonate electrolyte. This allows use of ceramic materials not generally considered compatible with a molten carbonate system. The amounts of the materials may vary, but are preferably used in a range of 40–45 vol% of the inert submicron particles, 5–30 vol% of the larger, crack attenuating ceramic particles with the balance being the plastic binder material.

4.2.2. Ceramic fibers

Fiber reinforced cements and concretes were developed not to obtain high strength materials, but in order to overcome the problems brought about by the low tensile strength and strain capacity of plain concrete. It was found that, although there were only modest improvements in strength, fiber additions greatly improved the "toughness" of concrete, that is, the total energy absorbed in breaking a specimen, and gave concrete with a considerable amount of apparent ductility. It was assumed that the main function of the fibers is to provide a crack arrest mechanism, that is, the fibers inhibit the propagation of cracks through the brittle matrix [42]. On this basis, $LiAlO_2$ and Al_2O_3 fibers have been used as reinforcement of the $LiAlO_2$ matrix to improve its mechanical properties. Ong and Hrdina [43] proposed a porous $LiAlO_2$ matrix reinforced with α-Al_2O_3 or γ-$LiAlO_2$ fibers, in the range of 5–50 vol% of the volume of the solids, with an average diameter of 1–50 μm and an average length greater than about 5 times the average diameter. Such matrices reduce matrix cracking upon loading with molten carbonates active electrolyte and provide high surface area over long term fuel cell operation. The toughening obtained is a microstructure strengthening of the electrolyte matrix and different from prior attempts of mechanical reinforcing by arresting of cracks by particles. In this case, fracture toughness is provided in the electrolyte matrix structure by crack deflection, that is cracks being attracted by the micro-fibers and propagating parallel or at right angles to them, and by the resistance to fiber pullout, that is the shear resistance of the fiber/matrix interface. Wake toughening, related to fiber pullout, occurs when fibers bridge across crack faces in the wake region of an extending crack providing further electrolyte matrix toughening. This combination of fracture toughness cannot be provided by large particles previously. The fibers are preferably in a random orientation and are of random lengths to provide

the best toughening effects. Networks of such fibers distribute stresses over large volumes and thereby strengthen the structure in a manner which cannot be achieved by particles. Hyun et al. [44] prepared γ-$LiAlO_2$ matrices containing 10–30 wt% Al_2O_3 or γ-$LiAlO_2$ fibers. Regarding the flexural strength, the optimum length and content of the Al_2O_3 fibers were 250 μm and 20 wt%, respectively, as can be seen in Fig. 11. The strength of the γ-$LiAlO_2$ matrix reinforced with γ-$LiAlO_2$ fibers was higher by 20–40% in comparison with the Al_2O_3 fiber-reinforced matrix. They also found that Al_2O_3 fiber-reinforced matrix was completely corroded in molten carbonates, but γ-$LiAlO_2$ fiber-reinforced matrix not. Fibers of β-$LiAlO_2$ were fabricated by the reaction of $Al(OH)_3$ and LiOH in aqueous solution at about 100 °C, then transformed to γ-phase at 800 °C [45]. The $LiAlO_2$ fibers were single-crystal with length of 10–15 μm. The performance of a MCFC with the matrix reinforced with the γ-$LiAlO_2$ fibers showed remarkable stability and the γ-$LiAlO_2$ fibers and the reinforced matrix showed no degradation after the cell testing of about 1200 h including 20 heat cycles of start and stop. Nirasawa et al. [46] fabricated a stabilized matrix with α-$LiAlO_2$ as the electrolyte support material and with long α-Al_2O_3 fibers as the reinforcement. The performance of a MCFC with this matrix was stable for 7000 h. The matrix degradation, such as the particle growth during cell operation and matrix cracking, did not occur in this cell. Finally, Hyun et al. [47] investigated the microstructural variation and strengthening effects by lamination methods of Al_2O_3 fiber-reinforced γ-$LiAlO_2$ matrices. The strength of the Al_2O_3 fiber-reinforced matrix prepared by lamination was enhanced by 70% in comparison with the non-laminated matrix and the strength-directionality due to fiber-orientation also was removed. The strength of matrices laminated by triple-casting was higher than that of the double-cast matrix, but triple-cast matrix showed the directionality with the casting direction, and furthermore its porosity was less than 50%. Although the strength of matrices laminated by double-casting was slightly less than that of matrices laminated by hot-pressing, the double-casting method was evaluated to be more efficient laminating process in MCFC matrix processing. Although Al_2O_3 fibers improve the mechanical strength, in addition to the high cost, problems regarding the use of Al_2O_3 fibers as reinforcing material in $LiAlO_2$ matrices are their insufficient long-term stability in molten carbonates at operating temperature, and the loss of electrolyte by the reaction of Li_2CO_3 with the Al_2O_3 fibers [48].

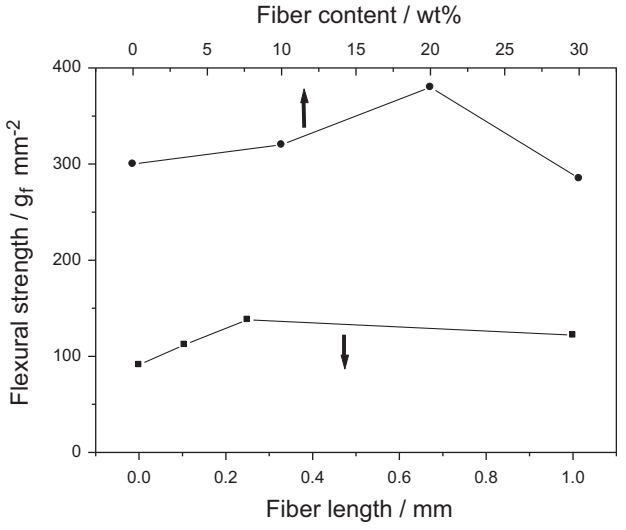

Fig. 11. Flexural strength vs. fiber content (matrix heat-treated at 1000 °C for 2 h) and vs. fiber length (matrix heat-treated at 650 °C for 2 h, 20 wt%, traverse direction).

4.3. Rod- and needle- shaped γ-LiAlO2 particles

Rod- and needle-shaped γ-$LiAlO_2$ single crystals, superior to polycrystalline fibers regarding their chemical and thermal stability and mechanical strength, have been considered as new material for reinforcing the MCFC matrix. Besides their property excellence, rod-shaped single crystals may also be uniformly dispersed inside the matrix even via tape casting [49]. Saeki and Watanabe [50] and Saeki et al. [51] synthesized rod- and needle-shaped γ-$LiAlO_2$ particles and tested their stability in molten carbonates at 650 °C. Rod-shaped β-$LiAlO_2$ particles (1.5 μm in diameter and 13–14 μm in length) were obtained in the LiOH–Al_2O_3–NaOH system at a molar ratio of 43.0:10.8:46.2, while needle-shaped β-$LiAlO_2$ particles (diameter of 0.9 μm, length of 10.4 μm) were achieved in the LiOH–Al_2O_3–$Al(OH)_3$–NaOH system at a molar ratio of 41.7:7.3: 6.2: 44.8. Rod- and needle-shaped β-$LiAlO_2$ crystals were converted to γ-$LiAlO_2$ crystals without morphology change by thermal treatment at 700–1000 °C for 10–30 h. Both rod-shaped and needle-shaped γ-$LiAlO_2$ crystals underwent no deformation by the heat treatment in molten carbonates at 650 °C for 1000 h. Kwon and Park [52] investigated the effect of precursors on the morphology of lithium aluminate, prepared by a hydrothermal treatment method. Lithium butoxide–aluminum butoxide system gave mostly rod-like β-$LiAlO_2$ crystal. As the length of alkoxy group decreases, the fraction of plate shape crystals was increased and boehmite was the dominant crystal phase. Needle-shape β-$LiAlO_2$ was produced from lithium nitrate-aluminum butoxide-sodium hydroxide system with the mole ratio of 6:1:3, respectively. β-$LiAlO_2$ prepared by hydrothermal treatment was transformed to γ-$LiAlO_2$ at 750–850 °C. The specific surface area of γ-$LiAlO_2$ powders was $> 10\ m^2\ g^{-1}$. On these bases, Hyun et al. [49], Kim et al. [53] and Choi et al. [54] used rod-shaped γ-$LiAlO_2$ to improve the strength of the matrix. They prepared rod-shaped β-$LiAlO_2$ particles from LiOH and α-Al_2O_3, according to the following reaction:

$$2LiOH + \alpha\text{-}Al_2O_3 \rightarrow 2\beta\text{-}LiAlO_2 + H_2O$$

using NaOH as a flux and reaction promoter. For the synthesis of γ-$LiAlO_2$ particles by phase transition of β to γ form, the rod-shaped β-$LiAlO_2$ particles were heat treated at 700–800 °C for 0.5–20 h. The addition of carbon and ammonium carbonate effectively reduces the time of synthesizing rod-shaped γ-$LiAlO_2$ particles without introducing any

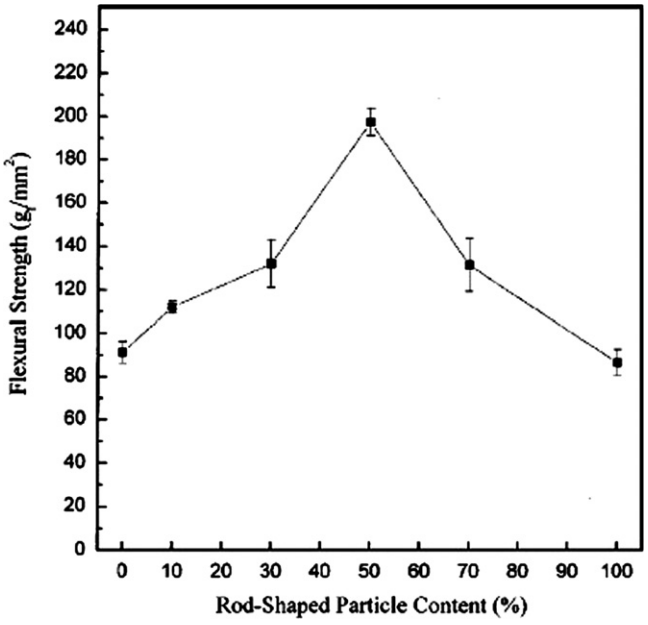

Fig. 12. Flexural strength vs. rod-shaped particle content. Reprinted from Ref. [49] copyright 2001, with permission from Springer.

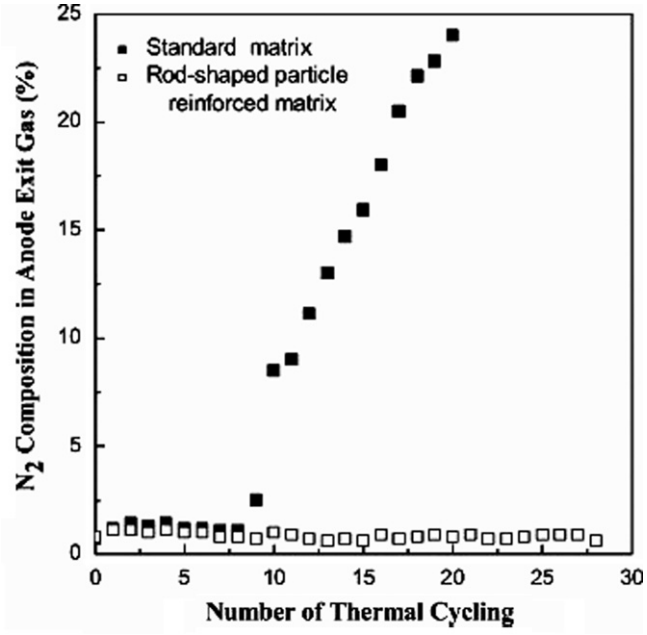

Fig. 13. N_2 cross-over in single cells with rod-shaped particle reinforced matrix and standard matrix due to thermal cycling. Reprinted from Ref. [53] copyright 2004, with permission from Elsevier.

residual products [52]. Most of the rod-shaped β-/γ-$LiAlO_2$ particles are 1 μm in diameter and 10–15 μm long (aspect ratio of 10–15). The flexural strength of $LiAlO_2$ matrices reinforced with rod-shaped particles was measured as shown in Fig. 12. The maximum strength was obtained when adding 50 wt% rod shaped particles, and its strength ($197.6 g_f\,mm^{-2}$) was increased more than twice than that rod shaped particle-free matrix ($91 g_f\,mm^{-2}$). This effect was explained considering that the 2D distribution of a lot of rod-shaped particles might prevent cracks from propagating. The occurrence of cracks in the matrices can be determined by measuring the amount of gas cross-over. To evaluate the occurrence of cracks, the N_2 gas composition in the anode exit gas was monitored following thermal cycles (see Fig. 13). For standard matrices, N_2 gas cross-over is under 3% during the first nine thermal cycles. N_2 gas cross-over increases appreciably, however, after the 10th thermal cycle (8.5%). This suggests occurrence of cracks in the matrices. The incidence of such cracks increases with increasing the number of thermal cycles (N_2 cross-over 23% after the 20th cycle). On the other hand, for rod-shaped particle reinforced matrices, N_2 crossover remains below 3% during 28 thermal cycles, indicating that such reinforced matrices have superior thermal stability to that of a standard matrix.

4.4. Metal wire mesh

Kim et al. [55] reinforced the electrolyte matrix with metal wire mesh. Stainless steel-40 (AISI type no. 304) mesh which a diameter in the range of 0.30–0.33 mm was used as metal wire mesh. To evaluate the durability of each matrix, long term single cell tests were used. The results from the cell tests are shown in Fig. 14. N_2 cross-over of pure matrix single cell have increased significantly after about 900 h operating time and an increase of internal resistance (IR) and a decline of cell performance also occurred at once. On the other hand, in the two mesh matrix long term single cells, significant increase of N_2 cross-over was not observed and it was maintained in 0.1–0.9% constantly during operation time. Moreover, internal resistance and cell performance was stable.

4.5. Additives with low melting point

Where the reinforcements act as crack arrestors or deflectors, as in the case of ceramic fibers and particles, unsintered ceramic particles in the matrices are only weakly bonded with the impregnated carbonate. As a result, thermal stress alone can still generate microcracks in the matrix. Microcracks can also be generated by mechanical stress, particularly during the start-up after binder burnout. Although these microcracks are not of a size which allows fuel and oxidant gas cross leakage during initial fuel cell operation, they can eventually propagate to larger sizes, causing increased cross leakage after several thermal cycles. The aforesaid microcracking can be reduced by the use of reinforcements which enhance bonding. Thus, dispersed metal powder phase (Al, Zn) reinforcements can sinter to provide higher strength during both start-up and operation. A higher strength is essential for reducing microcracking. Low melting points of the metal phases, (about 660 °C for Al and about 419 °C for Zn) are required for producing the sintering. The low melting point of the additive allows the particles of the additive material to sinter together or with the ceramic

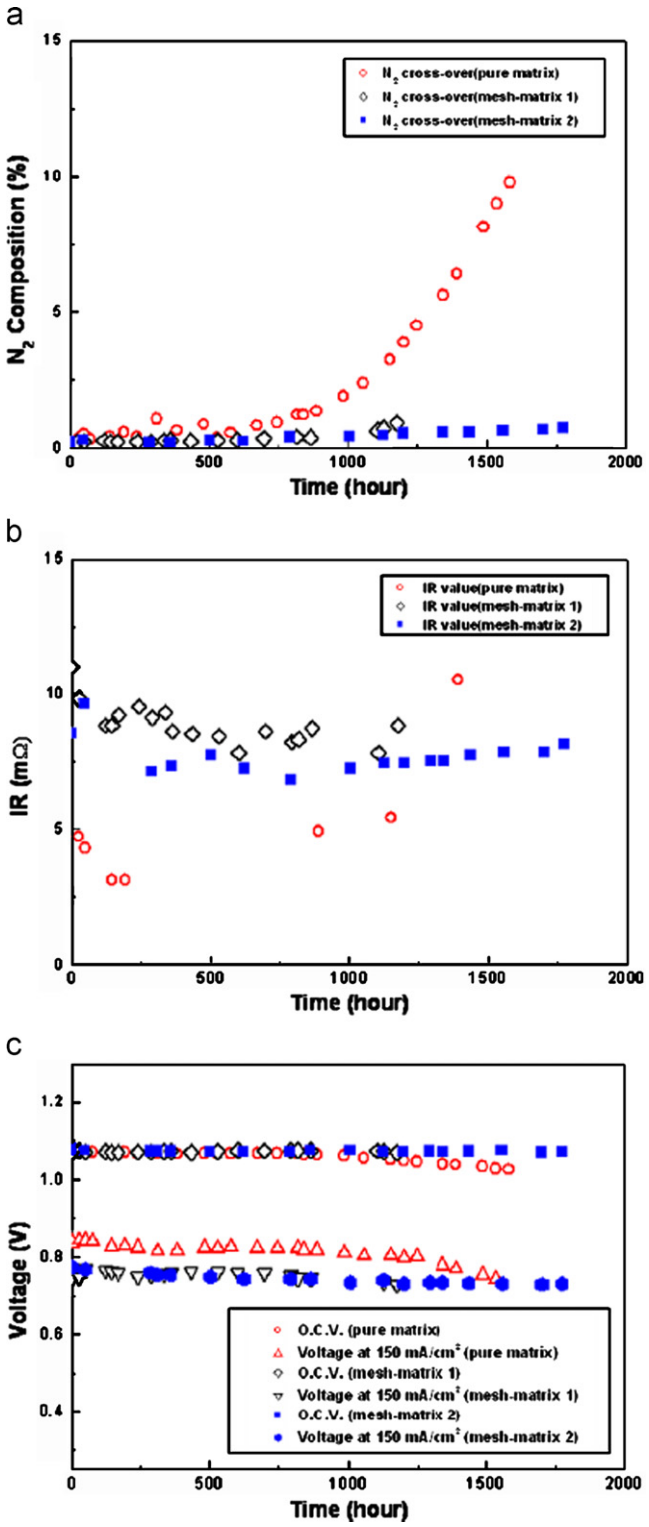

Fig. 14. Variation of (a) N_2 cross-over, (b) IR value and (c) O.C.V. and performance at 150 mA cm^{-2} current density. in single cells with mesh-reinforced matrices and additive-free matrix. Reprinted from Ref. [55] copyright 2010, with permission from Elsevier.

particles of the support material. This permits the bonding of these materials in situ at or below the operating temperature of the fuel cell. In a US patent, Huang and Yuh [56] proposed the use of aluminum, having a relatively low melting point and a relatively high thermal coefficient of expansion, for strengthening the matrix, in an amount from 3 to 45 vol% and being formed from raw particles having a size in the range 0.1–20 μm. Al reacts with the carbonate melt to form $LiAlO_2$, according to the following reaction:

$$2Al + Li_2CO_3 + 3/2O_2 \rightarrow 2LiAlO_2 + CO_2 \quad (4)$$

Li_2CO_3, Li/KCO_3, $Li/NaCO_3$ or other Li-containing precursors (formate, acetate, etc.) were also added to the matrix. The presence of these Li containing materials compensates Li loss during $LiAlO_2$ formation and prevents a Li-ion shortage in the matrix. In the same way, Lee et al. [57] and Kim et al. [58] used Al/Li_2CO_3 particles as reinforcing materials in γ-$LiAlO_2$ and α-$LiAlO_2$ powders, respectively. In both cases the mechanical strength of the Al/Li_2CO_3 particle-reinforced $LiAlO_2$ matrix increased in comparison with that of the conventional $LiAlO_2$ matrix. In the same way, the long-term stability of MCFC performance using Al-reinforced-$LiAlO_2$ matrices is superior to that of MCFCs with non-reinforced standard matrices. A decay in the performance of MCFCs with a non-reinforced matrix after an operation time of 700 h was observed. Both the internal resistance and N_2 crossover increased, indicating that the performance decay was due mainly to crack formation in the non-reinforced matrix. The requirement of Li_2CO_3 addition to Al is demonstrated comparing Fig. 15a and b [58]. As can be seen in Fig. 15a, the performance of the cell incorporating the Al (3 mm, 30 wt%)-reinforced matrix without additional Li_2CO_3 starts to decay after an operation time of 750 h. Although the degree of N_2 crossover is almost stable, the internal resistance increases steeply after operation for 750 h. The consumption of Li ions of the eutectic Li/K carbonate melt changes the composition of the liquid electrolyte, leading to an increase in the internal resistance without an increase in N_2 crossover. By post-test analyses many cracks were observed in the non-reinforced matrix but no cracks were found in the Al-reinforced matrix, attesting the different degradation mechanisms of the two cells. Conversely, Fig. 15b indicates that the cell performance of the Al-reinforced matrix incorporating Li_2CO_3 was initially lower, but after 1000 h operation, it attained near the initial performance of the non-reinforced cell. The cell with the Al/Li_2CO_3-reinforced matrix operated for 2000 h exhibiting a stable performance of 0.78 V at a current density of 150 mA cm^{-2} without an increase in the N_2 crossover or the internal resistance. These studies showed that the addition of Al and Li_2CO_3 to the matrix is an effective means of increasing the mechanical strength of the matrix and increasing the cell stability, while providing good cell performance. Unfortunately, the Li_2CO_3 particles incorporated in the matrix can cause large voids to form, which can be associated with a massive gas cross-over through the cracks formed in the Al-reinforced $LiAlO_2$ matrix. Li_2CO_3 particles added to Al-reinforced matrix, can lead to cross-over failure as numerous pores/cracks propagate in the matrix. To suppress the lithium-ion shortage in the Al-reinforced matrix by

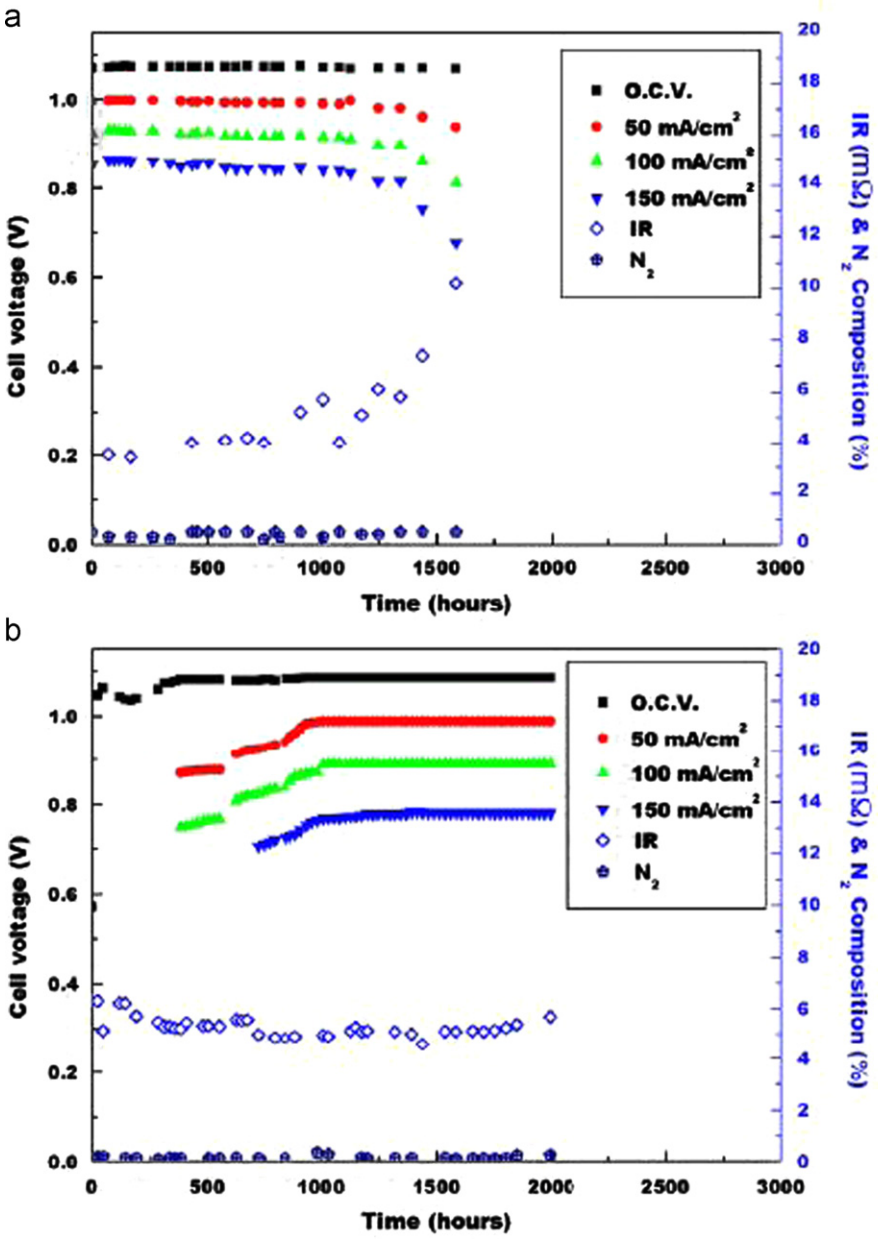

Fig. 15. Performance of single cells incorporating (a) Al (3 mm, 30 wt%)-reinforced matrix and (b) Al (3 mm, 30 wt%)/Li_2CO_3-reinforced matrix. Reprinted from Ref. [58] copyright 2009, with permission from Elsevier.

employing a low-melting-point lithium source without void formation, different pathways have been explored, such as Li_2CO_3 incorporated into the cathode so that the lithium will migrate into the Al-reinforced matrix, and LiOH (melting point 462 °C) stored in the cathode channel of separator [59,60]. Compared to the other lithium content pathways, the pathway with LiOH was the more suitable to improve the mechanical stability of the matrix, allowing the cell to operate for 4060 h. The low melting-point LiOH prevented the formation of voids in the matrix, and no deterioration of the single cell was observed.

Ham et al. [61,62] observed that the mechanical strength of a $LiAlO_2$ matrix can be increased by the addition of B_2O_3 (melting point 450 °C). The enhancement of mechanical strength in the B_2O_3-additivated matrix was mainly attributed to the formation of a Li_2AlBO_4 phase by the reaction between B_2O_3 and $LiAlO_2$. The new phase promotes the sintering between the $LiAlO_2$ particles, thereby increasing the strength of the matrix. In addition, since the Li_2AlBO_4 phase is stable at a MCFC operation temperature and carbonate environment, it enables the MCFC to work for a long time. Moreover, unlike Al, since the strength of the matrix can be increased before the melting of the electrolyte, it is possible to improve the resistance to the mechanical stress due to the non-uniformity of the surface pressure during the pretreatment of the molten carbonate fuel cell. This considerably contributes to improvement of durability of the molten carbonate fuel cell.

4.6. Aluminum acetylacetonate ($C_{15}H_{21}AlO_6$) as a sintering aid

Aluminum acetylacetonate has been investigated as a sintering aid for the in situ sintering of $LiAlO_2$ matrices [63]. At or above 420 °C, $C_{15}H_{21}AlO_6$ changes to Al_2O_3 and, according to reaction (2), reacts with Li_2CO_3 in the electrolyte to produce γ-$LiAlO_2$. This reaction product forms necks between matrix particles. Necks grow with increasing sintering time and, correspondingly, the mechanical strength of the matrix also increases. The mechanical strength plotted against sintering time for three different electrolyte matrices is shown in Fig. 16 [63]. Two of these matrices were made of coarse γ-$LiAlO_2$ powder (LSA-50), one with $C_{15}H_{21}AlO_6$ and the other without, and the third was made of a mixture of fine γ-$LiAlO_2$ powder (HSA-10), LSA-50, and alumina fibers also using $C_{15}H_{21}AlO_6$ as a sintering aid. When the LSA-50 matrices are compared, the role of the aluminum salt in the process of sintering of electrolyte matrices can be clearly observed. The mechanical strength shows an abrupt increase starting at a sintering time of about 100 h until it levels off at about 250 h for the one with aluminum salt, while there is almost no variation of mechanical strength with sintering time for the other. The composite matrix with aluminum salt shows a similar trend as the corresponding LSA-50 matrix, but has higher strength at all sintering times. The porosity of the matrices fabricated with $C_{15}H_{21}AlO_6$ is in the range acceptable for use in MCFCs.

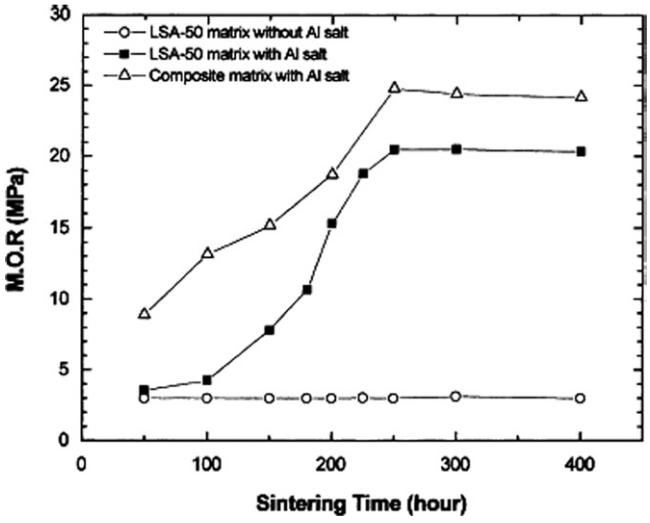

Fig. 16. Rupture modulus vs. sintering time for different matrices, with and without Al salt. Reprinted from Ref. [63] copyright 2001, with permission from Elsevier.

5. Conclusions

Lithium aluminate is commonly used as the electrolyte support in MCFCs. Its long term stability in MCFC environment is a key requirement in order to attain more than 40,000 h of MCFC life. Both α- and γ-$LiAlO_2$ phases have been tested as electrolyte matrix materials in MCFCs. At 650 °C and in CO_2 atmosphere α-$LiAlO_2$ seems to be more stable than γ-$LiAlO_2$ in both Li/K and Li/Na carbonates. Both α- and γ-$LiAlO_2$ are less soluble in Li/K than in Li/Na carbonates, so from the point of view of the matrix it should be better to use the Li//K carbonate

Table 3
Methods for improving the mechanical strength of the $LiAlO_2$ matrix in molten carbonates.

Method	Material	Effect	Refs.
Addition of metallic alloys	1–6 vol% FeCrAlCo	Not specified	37
Addition of large particles	10 vol% Al_2O_3 (size > 100 μm) 5–30 vol% $LiAlO_2$ or Al_2O_3 (size > 50 μm)	Formation of a multitude of tiny discontinuous cracks, rather than of one or more large thru-cracks	40 41
Addition of fibers	5–50 vol% $LiAlO_2$ (length 30–1000 μm) or Al_2O_3 (length 150 μm) 20 vol% $LiAlO_2$ or Al_2O_3 (length 250 μm) γ-$LiAlO_2$ (length 10–15 μm) Al_2O_3	Fracture toughness is provided by crack deflection, i.e. cracks being attracted by the micro-fibers and propagating parallel or at right angles to them, and by the resistance to fiber pullout, i.e. is the shear resistance of the fiber/matrix interface	41 44 45 46,47
Addition of rod-shaped γ-$LiAlO_2$ particles	50 vol% (optimum) rod-shaped γ-$LiAlO_2$ 1 μm in diameter and 10–15 μm long (aspect ratio 10–15)	The 2D distribution due to the addition of a lot of rod-shaped particles prevents cracks from propagating	49,53,54
Addition of metal wire mesh	Stainless steel-40 (AISI type No. 304) mesh which a diameter in the range of 0.30–0.33 mm	Not specified	55
Use of additives with low melting point	3–45 vol% Al (0.1–50 μm) + Li_2CO_3 5 vol% Al (3,20,50 μm) + Li_2CO_3 30 wt% Al (3 μm) + Li_2CO_3 Al + LiOH B_2O_3	The low melting point of the additive allows the particles of the additive material to sinter together or with the ceramic particles of the support material. This permits the bonding of these materials in situ at or below the operating temperature of the fuel cell	56 57 58 59,60 61,62
Use of $C_{15}H_{21}AlO_6$ as a sintering aid	$C_{15}H_{21}AlO_6$ (0.1 μm)	$C_{15}H_{21}AlO_6$ reacts with Li_2CO_3 forming $LiAlO_2$, which gives rise to neck formation between matrix particles	63

melt. However, considering its negative effect on NiO cathode and DIR-MCFC anode stabilities, the tendency is to substitute K_2CO_3 in the electrolyte with Na_2CO_3. Indeed, the NiO cathode is more soluble in K_2CO_3 than in Na_2CO_3 [64], and steam reforming catalysts are poisoned by alkali carbonate electrolytes, and this effect is most pronounced for K and less pronounced for Na [65], owing to the high vaporization of the K species. The effect of additives on inhibiting particle growth and phase transformation of $LiAlO_2$ has been investigated. It was found that zirconia and potassium tungstate powders can inhibit both $LiAlO_2$ particle growth and phase transformation.

Different methods have been utilized to increase the mechanical strength of $LiAlO_2$ matrices, as summarized in Table 3. Second-phase crack attenuators, such as large $LiAlO_2$ particles, have been used but, these materials have not promoted the desired strengthening and longevity of the matrix. Regarding the use of ceramic fibers, they improved the mechanical strength, however, the main drawback of alumina fiber reinforcement is that commercial ceramic fiber is costly and not sufficiently stable in melted alkali carbonate electrolytes. Rod-shaped $LiAlO_2$ particles, which are superior to fibers in terms of their chemical and thermal stability and mechanical strength have been developed as a new material for reinforcing the MCFC matrix. Nevertheless, owing to their cost and complex preparation methods, these materials do not yet meet the commercialization requirements of the MCFC system. The most effective and economical solution seems to be the use of $Al+Li_2CO_3$/LiOH additives. The low melting point of aluminun allows the particles of the additive material to react with the carbonate melt to form $LiAlO_2$ and, then, to sinter with the ceramic particles of the support material. This permits the bonding of these materials in situ at or below the operating temperature of the fuel cell. The addition of Li containing materials compensates Li loss during $LiAlO_2$ formation and prevents a Li-ion shortage in the matrix.

References

[1] M. Bischoff, Large stationary fuel cell systems: status and dynamic requirements, Journal of Power Sources 154 (2006) 461–466.

[2] Q.M. Nguyen, Technological status of nickel oxide cathodes in molten carbonate fuel cells–A review, Journal of Power Sources 24 (1988) 1–19.

[3] B.C.H. Steele, Material science and engineering: the enabling technology for the commercialisation of fuel cell systems, Journal of Materials Science 36 (2001) 1053–1068.

[4] A.L. Dicks, Molten carbonate fuel cells, Current Opinion in Solid State and Materials Science 8 (2004) 379–383.

[5] C. Yuh, M. Farooque, Fuel cells–molten carbonate fuel cells. Materials and life considerations, Encyclopedia of Electrochemical Power Sources (2009) 497–507.

[6] S. Freni, S. Cavallaro, M. Equino, D. Ravida, N. Giordano, Lifetime-limiting factors for a molten carbonate fuel cell, International Journal of Hydrogen Energy 19 (1994) 337–341.

[7] H. Morita, M. Kawase, Y. Mugikura, K. Asano, Degradation mechanism of molten carbonate fuel cell based on long-term performance: long-term operation by using bench-scale cell and post-test analysis of the cell, Journal of Power Sources 195 (2010) 6988–6996.

[8] E. Antolini, The stability of molten carbonate fuel cell electrodes: a review of recent improvements, Applied Energy 88 (2011) 4274–4293.

[9] H.J. Choi, J.J. Lee, S.H. Hyun, H.C. Lim, Fabrication and performance evaluation of electrolyte-combined α-LiAlO2 matrices for molten carbonate fuel cells, International Journal of Hydrogen Energy 36 (2011) 11048–11055.

[10] J.P.P. Huijsmans, G.J. Kraaij, R.C. Makkus, G. Rietveld, E.F. Sitters, H.Th.J. Reijers, An analysis of endurance issues for MCFC, Journal of Power Sources 86 (2000) 117–121.

[11] M. Marezio, J.P. Remeika, High-pressure synthesis and crystal structure of α-$LiAlO_2$, Journal of Chemical Physics 44 (1966) 3143–3144.

[12] M. Marezio, The crystal structure and anomalous dispersion of γ-$LiAlO_2$, Acta Crystallographica 19 (1965) 396–400.

[13] J. Thery, A.M. Lejus, D. Briancon, R. Collongues, Structure and properties of alkaline aluminates, Bulletin de la Societe chimique de France (1961) 973–975.

[14] H.J. Byker, I. Eliezer, N. Eliezer, R.A., Howald, C. Verwolf, P. Viswanadham, in: High Temperature Fuel Cell Research and Development, Final Report for DOE Contract no. EC-77-C-03-1485 for the period June 1977–September 1978, MT.

[15] V. Danek, M. Tarniowy, L. Suski, Kinetics of the phase transformation in $LiAlO_2$ under various atmospheres within the 1073–1173 K temperatures range, Journal of Materials Science 39 (2004) 2429–2435.

[16] S. Terada, I. Nagashima, K. Higaki, Y. Ito, Stability of $LiAlO_2$ as electrolyte matrix for molten carbonate fuel cells, Journal of Power Sources 75 (1998) 223–229.

[17] H. Sotouchi, Y. Watanabe, T. Kobayashi, M. Murai, Mechanism of crystal growth of lithium aluminate particles in molten lithium and potassium carbonates, Journal of the Electrochemical Society 139 (1992) 1127–1130.

[18] M. Murai, K. Takizawa, K. Soejima, H. Sotouchi, Crystal growth of γ-lithium aluminate in molten Li/K carbonates, Journal of the Electrochemical Society 143 (1996) 2776–2783.

[19] L. Zhou, H. Huaxin, B. Yi, Sintering behavior of porous α-lithium aluminate matrices in molten carbonate fuel cells at high temperature, Journal of Power Sources 164 (2007) 24–32.

[20] K. Takizawa, A. Hagiwara, The transformation of $LiAlO_2$ crystal structure in molten Li/K carbonate, Journal of Power Sources 109 (2002) 127–135.

[21] K.Y. Patil, S.P. Yoon, J. Han, T.H. Lim, S.W. Nam, J.H. Oh, S.A. Hong, Phase stabilities in molten Li/K carbonates fuel cells: thermodynamic calculations and experimental investigations, Journal of Materials Science 46 (2011) 2557–2567.

[22] N. Tomimatsu, H. Ohzu, Y. Akasaka, K. Nakagawa, Phase stability of $LiAlO_2$ in molten carbonate, Journal of the Electrochemical Society 144 (1997) 4182–4186.

[23] K. Tanimoto, M. Yanagida, T. Kojima, Y. Tamiya, H. Matsumoto, Y. Miyazaki, Long-term operation of small sized single molten carbonate fuel cells, Journal of Power Sources 72 (1998) 77–82.

[24] V.S. Batra, S. Maudgal, S. Bali, P.K. Tewari, Development of alpha lithium aluminate matrix for molten carbonate fuel cell, Journal of Power Sources 112 (2002) 322–325.

[25] S. Terada, K. Higaki, I. Nagashima, Y. Ito, Stability and solubility of electrolyte matrix support material for molten carbonate fuel cells, Journal of Power Sources 83 (1999) 227–230.

[26] S.D. Kim, S.H. Hyun, M.Y. Shin, T.H. Lim, S.A. Hong, H.C. Lim, Phase and microstructure stabilities of $LiAlO_2$ in molten Li/Na carbonate for molten carbonate fuel cells, Journal of Power Sources 143 (2005) 24–29.

[27] L. Suski, M. Tarniowy, The phase stability of solid $LiAlO_2$ used for the electrolyte matrix of molten carbonate fuel cells, Journal of Materials Science 36 (2001) 5119–5124.

[28] Y. Fujita, T. Nishimura, T. Yagi, M. Matsumura, Degradation of the components in molten carbonate fuel cells with Li/Na electrolyte, Electrochemistry 71 (2003) 7–13.

[29] E. Yasumoto, K. Hatoh, T. Gamo, Particle growth behaviour of $LiAlO_2$ containing ZrO_2 in Li/Na carbonate electrolytes, Journal of Power Sources 71 (1998) 159–163.

[30] S. Terada, K. Higaki, I. Nagashima, Y. Ito, Addition of potassium tungstate to the electrolyte of a molten carbonate fuel cell, Journal of Power Sources 83 (1999) 178–185.
[31] C. Alvani, E. Roncari, Preparation and characterization of γ-LiAlO2 tiles for the molten carbonate fuel cells, High Temperatures–High Pressures 20 (1988) 247–250.
[32] J.J. Seo, S.T. Kuk, K. Kim, Thermal decomposition of PVB (polyvinyl butyral) binder in the matrix and electrolyte of molten carbonate fuel cells, Journal of Power Source 69 (1997) 61–68.
[33] S. Masia, P.D. Calvert, W.E. Rhine, H.K. Bowen, Effect of oxides on binder burnout during ceramics processing, Journal of Materials Science 24 (1989) 1907–1912.
[34] D.R. Wall, H.Y. Shon, Removal of carbonaceous residue with wet hydrogen in greensheet processing for multilayer ceramic module. I, residue formation and intrinsic chemical kinetics, Journal of the American Ceramic Society 73 (1990) 2944–2952.
[35] H. Lin, L. Zhou, C. He, L. Kong, E. Zhang, B. Yi, A study on the dependence of the micro-pore configurations on the volatilization and the burn processes of the organic compounds in the matrix of molten carbonate fuel cells, Electrochimica Acta 47 (2002) 1451–1459.
[36] V.S. Batra, S. Bali, S. Venkatesh, Fabrication of porous components for molten carbonate fuel cell, Ceramics International 29 (2003) 547–553.
[37] R.N. Arendt, J. Curran, Process of making electrolyte structure for molten carbonate fuel cells, US Patent no. 4,216,278, 1980.
[38] K.T. Faber, A.G. Evans, Crack deflection processes-I. Theory, Acta Metallurgica 31 (1983) 565–576.
[39] C.Y. Yuh, C.M. Haung, R. Johnsen, Carbonate fuel cell matrix strengthening, DOE/MC/815 12-96/C0609.
[40] C.L. Bushnell, L.J. Bregoli, C.R. Schroll, Electrolyte matrix for molten carbonate fuel cells, US Patent no. 4,322,482, 1982.
[41] R.W. Vine, C.R. Schroll, C.A. Reiser, Molten carbonate fuel cell matrix tape and assembly method, US Patent no. 4,538,348, 1985.
[42] S. Mindess, The fracture of fiber-reinforced and polymer impregnated concretes, International Journal of Cement Composites and Lightweight Concrete 2 (1980) 3–11.
[43] E.T. Ong, K.E. Hrdina, Molten carbonate fuel cell electrolyte toughening, US Patent no. 5,316,555, 1994.
[44] S.H. Hyun, K.H. Baek, S.-A. Hong, Preparation of fiber-reinforced γ-LiAlO2 matrixes by the tape casting method, Journal of the Korean Ceramic Society 34 (1997) 303–313.
[45] K. Suzuki, T. Kakihara, Y. Yamamasu, T. Sasa, Advanced fabrication process of $LiAlO_2$ fiber and its application to porous matrix for molten carbonate fuel cell, Materials Research Society Symposium Proceedings 371 (1995) 297–302.
[46] H. Nirasawa, T. Kawachi, T. Ogawa, M. Hori, N. Tomimatsu, K. Nakagawa, H. Ohzu, Y. Yamazaki, Energy Conversion Engineering Conference, IECEC 96. Proceedings of the 31st Intersociety 2, 1996,pp. 1132–1137.
[47] S.H. Hyun, S.C. Cho, S.A. Hong, Strengthening of fiber-reinforced γ-LiAlO2 matrixes for molten carbonate fuel cells by lamination, Journal of the Korean Ceramic Society 36 (1999) 107–115.
[48] M. Murai, K. Takizawa, K. Soejima, H. Sotouchi, Lithiation of alumina in molten Li/K carbonates, Journal of the Electrochemical Society 143 (1996) 3456–3462.
[49] S.-H. Hyun, S.C. Cho, J.-Y. Cho, D.-H. Ko, Reinforcement of molten carbonate fuel cell matrixes by adding rod-shaped γ-$LiAlO_2$ particles, Journal of Materials Science 36 (2001) 441–450.
[50] G. Saeki, A. Watanabe, Modification from rod-shaped β-$LiAlO_2$ crystals to γ-$LiAlO_2$ crystals without morphology change and stability of γ-$LiAlO_2$ crystals in alkali carbonates, Journal of the Ceramic Society of Japan 102 (1994) 565–569.
[51] G. Saeki, H. Takahashi, A. Watanabe, Synthesis of needle-shaped γ-$LiAlO_2$ crystals by using $LiOH$-Al_2O_3-$Al(OH)_3$-$NaOH$ system as the raw material, Journal of the Ceramic Society of Japan 104 (1996) 221–225.
[52] S.W. Kwon, S.B. Park, Effect of precursors on the morphology of lithium aluminate prepared by hydrothermal treatment, Journal of Materials Science 35 (2000) 1973–1978.
[53] S.D. Kim, S.H. Hyun, T.H. Lim, S.A. Hong, Effective fabrication method of rod-shaped γ-$LiAlO_2$ particles for molten carbonate fuel cell matrices, Journal of Power Sources 137 (2004) 24–29.
[54] H.J. Choi, M.Y. Shin, S.H. Hyun, H.C. Lim, Optimization of rod-shaped γ-LiAlO2 particle reinforced MCFC matrices by aqueous tape casting, Journal of the Korean Ceramic Society 46 (2009) 282–287.
[55] J.E. Kim, J.H. Han, S.P. Yoon, S.W. Nam, T.H. Lim, H. Kim, Mechanical properties of the lithium aluminate matrix for MCFC reinforced with metal oxide materials, Current Applied Physics 10 (2010) 573–576.
[56] C.M. Huang, C. Yuh, Electrolyte matrix for molten carbonate fuel cells, US Patent no. 5,869,203, 1999.
[57] J.J. Lee, H.J. Choi, S.H. Hyun, H.C. Im, Characteristics of aluminum-reinforced γ-$LiAlO_2$ matrices for molten carbonate fuel cells, Journal of Power Sources 179 (2008) 504–510.
[58] J.E. Kim, K.Y. Patil, J. Han, S.P. Yoon, S.W. Nam, T.H. Lim, S.A. Hong, H. Kim, H.C. Lim, Using aluminum and Li_2CO_3 particles to reinforce the α-$LiAlO_2$ matrix for molten carbonate fuel cells, International Journal of Hydrogen Energy 34 (2009) 9227–9232.
[59] K.Y. Patil, S.P. Yoon, J. Han, T.H. Lim, S.W. Nam, I.H. Oh, S.A. Song, A study of alternative matrix materials and their reinforcement for molten carbonate fuel cells, in: 218th ECS Meeting, Las Vegas, NV, 2010.
[60] K.Y. Patil, S.P. Yoon, J. Han, T.H. Lim, S.W. Nam, J.H. Oh, The effect of lithium addition on aluminum-reinforced α-LiAlO2 matrices for molten carbonate fuel cells, International Journal of Hydrogen Energy 36 (2011) 6237–6247.
[61] H.C. Ham, S.P. Yoon, J. Han, S.W. Nam, T.H. Lim, S.A. Hong, Development of reinforced matrix for molten carbonate fuel cells by using sintering aids, ECS Transactions 5 (2007) 445–449.
[62] H.C. Ham, S.A. Hong, I.H. Oh, T.H. Lim, S.W. Nam, S.P. Yoon, J. Han, J. Lee, H.J. Kim, E.A. Cho, K.S. Lee, H.Y. Ha, S.Y. Lee, Reinforced matrix for molten carbonate fuel cell and method for preparing the same, US Patent no. 7,790,327, 2010.
[63] I. Lee, W. Kim, Y. Moon, H. Lim, D. Lee, Influence of aluminum salt addition on in situ sintering of electrolyte matrices for molten carbonate fuel cells, Journal of Power Sources 101 (2001) 90–95.
[64] K. Ota, S. Mitsushima, S. Kato, S. Asano, H. Yoshitake, N. Kamiya, Solubilities of nickel oxide in molten carbonate, Journal of the Electrochemical Society 139 (1992) 667–671.
[65] K. Sugiura, M. Soga, M. Yamauchi, K. Tanimoto, Volatilization behavior of Li/Na carbonate as an electrolyte in MCFC, ECS Transactions 12 (2008) 355–360.